INFLUENCE OF ANTIBIOTIC ADSORPTION ON BIOCIDAL ACTIVITIES OF SILVER NANOPARTICLES

R.Elayaperumal [1], A.Vanitha[2], S.Suguna[3], M.Deepa[4]

Assistant professor,

[1]*Department of chemistry ,Dhanalakshmi Srinivasan College of Arts & Science for Women(Autonomous)*

Perambalur

ABSTRACT

Exorbitant utilization of anti-microbials has presented two significant difficulties in open medical care. One of them is related with the improvement of multi-drug obstruction while the other one is connected to results. In the current examination, the writers report an imaginative way to deal with tackle the difficulties of multi-drug opposition and intense poisonousness of anti-toxins by utilizing anti-microbials adsorbed metal nanoparticles. Monodisperse silver nanoparticles (SNPs) have been blended by two-venture measure. In the initial step, SNPs were set up by compound decrease of AgNO3 with oleylamine and in the subsequent advance, oleylamine covered SNPs were stage moved into a fluid medium by ligand trade. Anti-toxins - antibiotic medication and kanamycin were additionally adsorbed on the outside of SNPs. Antibacterial exercises of SNPs and anti-toxin adsorbed SNPs have been researched on gram-positive (Staphylococcus aureus, Bacillus megaterium, Bacillus subtilis), and gram-negative (Proteus vulgaris, Shigella sonnei, Pseudomonas fluorescens) bacterial strains. Synergistic impact of SNPs on antibacterial exercises of antibiotic medication and kanamycin has been noticed. Biocidal movement of antibiotic medication is improved by 0-346% when adsorbed on SNPs; while for kanamycin, the improvement is 110-289%. This synergistic impact of SNPs on biocidal exercises of anti-toxins might be useful in lessening their successful measurements.

INTRODUCTION

Anti-infection agents are generally used to treat irresistible illnesses brought about by pathogenic microorganisms [1]. Lately, genuine concerns have been raised by clinical experts towards the broad advancement of pathogenic living beings, which are impervious to different anti-toxins [2–4]. Another basic concern is not kidding results related with anti-microbial medications [5]. Non-target impacts of anti-infection agents can cause a scope of sicknesses like queasiness, the runs, unfavorably susceptible responses, fever to perilous illnesses like formationof kidney stones, unusual blood coagulating, liver transplantation, passing from intense liver disappointment, and so forth [6, 7]. To beat these restrictions of anti-microbials, pharmacologists are chipping away at substitute meds, which are neither inclined to the improvement of medication opposition nor experience the ill effects of genuine results related with customary anti-toxins [8, 9].

Antibacterial properties of metals are notable since old occasions [10]. They were generally utilized in preventive medical services throughout the entire existence of human civilisation [11]. Among respectable metals, silver has demonstrated a wide scope of biocidal exercises [12, 13].

Late improvement in nanoparticle innovation has additionally upgraded biocidal exercises of honorable metal nanoparticles [10]. Among honorable metals, silver has the most noteworthy antibacterial movement [14]. Because of this explanation, silver nanoparticles (SNPs) are currently generally utilized as antibacterial specialists in a scope of items like injury dressing, urinary track catheters, heart gadgets, effective gels, endotracheal breathing cylinders, dental embeds, etc [15].

There are a few reports on the size and portion subordinate harmfulness of SNPs in human cells [16–19]. In a new survey, Hadrup and Lam[17] have clarified different pathways of SNPs' poisonousness in human ordinary cells. Park et al. [18] and AshaRani et al. [19] have discovered that SNPs initiated cell harmfulness in human cells by DNA harm and chromosomal distortions. Harmfulness of SNPs to human cells is antagonistic and subsequently as of now, SNPs are administrated by skin implies just as salves under a basic edge fixation.

There are not many reports on synergistic impact of ordinary anti-infection agents on biocidal exercises of SNPs [20–22]. Filgueiras et al. [20] have revealed adsorption procedures of anti-toxins levofloxacin, antibiotic medication and benzyl penicillin on SNPs. Ghosh et al. [21] have shown synergistic antibacterial exercises of cinnamaldehyde adsorbed SNPs. Hwang et al. [22] have additionally detailed adsorption of ampicillin, chloramphenicol and kanamycin on SNPs. These reports have shown that adsorption of ordinary anti-microbials have synergistic impact on antimicrobial exercises of SNPs. Among customary anti-toxins, antibiotic medication and kanamycin are widely utilized for the treatment of different diseases [6, 23, 24]. The utilization of anti-infection agents is on decrease in light of the far and wide advancement of medication opposition in causative creatures [25, 26]. To defeat these disadvantages of thin focusing on anti-microbials, in this paper, we propose new definitions of these anti-microbial medications whose pharmacokinetic and toxicological impacts are now known. In this examination, we report amalgamation of uniform, monodispersed water-dispersible SNPs and anti-infection (antibiotic medication/kanamycin) adsorbed SNPs and their bactericidal exercises against pathogenic and non-pathogenic strains and attempted to comprehend the collaboration among traditional and nanoantibiotics.

MATERIALS AND METHODS

Silver nitrate ($AgNO_3$) (99.8%) and diphenyl ether were secured from S D Fine-Chem Limited. Oleylamine (70%) and pluronic F-127 were acquired from Sigma Aldrich. Outright ethanol, n-hexane (95%) and HPLC grade water were bought from Merck. All synthetic compounds were utilized as gotten minus any additional purification. Mueller Hinton Agar (MM019) and supplement stock (NM019) were bought from Sisco Research Laboratories. The gram-positive {[Staphylococcus aureus (S. aureus) (MTCC No. 9760)], [Bacillus megaterium (B. megaterium) (MTCC No. 428)], Bacillus subtilis (B. subtilis) (MTCC No. 441)}, and gram-negative {[Proteus vulgaris (P. vulgaris) (MTCC No. 426], [Shigella sonnei (S. sonnei) (MTCC

No.2957), [Pseudomonas fluorescens (P. fluorescens) (MTCC No. 1749)]} bacterial societies were gotten from IMTECH, Chandigarh, India. Anti-toxins antibiotic medication and kanamycin were bought from Himedia.

SYNTHESIS OF SNPs

In this study, we report synthesis of uniform, monodisperse SNPs by slow and controlled reduction of $AgNO_3$ with oleylamine [27]. Diphenyl ether (20 mL) was mixed with 15 mM oleylamine in a 100 mL round bottom flask, equipped with a magnetic stirrer, condenser and a thermometer. The mixture was heated to 200°C at 3°C/min. 3 mM $AgNO_3$ was added into the preheated diphenyl ether–oleylamine under continuous magnetic stirring. Colour of the mixture immediately turned blue when $AgNO_3$ was added into diphenyl ether–oleylamine. Strong surface plasmon resonance (SPR) was observed, indicating the nucleation of SNPs. It was refluxed for 30 min followed by ripening at 150°C for 4 h. The colloidal solution was then cooled down to room temperature, precipitated by ethanol and purified by precipitation–redispersion [27]. Oleylamine coating on SNPs surface renders them hydrophobic. For biomedical applications, SNPs must be water dispersible. To obtain water dispersible SNPs, in the second step, as-synthesised hydrophobic SNPs were phase transferred from n-hexane to water by the facile phase transfer protocols [28]. In brief, equal volume of aqueous pluronic F-127 was mixed with n-hexane solution of SNPs. Concentration of pluronic F-127 was kept such that the Ag: pluronic F-127 weight ratio was 1:0.5. Initially the organic phase of SNPs was well separated from the aqueous phase of pluronic. Upon magnetic stirring, both immiscible phases mixed with each other. The beaker was covered with a perforated aluminium foil tocontrol the evaporation of organic phase. It was stirred until the organic phase evaporated completely. To confirm the phase transfer of SNPs, n-hexane was poured into the aqueous solution of SNPs. On successful phase transfer, both aqueous and n-hexane phases would remain immiscible.

Antibiotic adsorbed SNPs were prepared by vortex mixing of 10 mL aqueous colloidal dispersion of SNPs with desired quantity of tetracycline or kanamycin for 12 h. The final concentration of SNPs in antibiotic adsorbed SNPs was adjusted to 250 ppm. The colloid was centrifuged at 12,000 RPM and supernal was removed. The final volume of nanoparticle suspension was readjusted to 10 mL by addition of ultrapure water. These stock solutions of antibiotic adsorbed SNPs were further used for the antibacterial activity test.

CHARACTERISATION OF SNPs

Growth of SNPs was monitored by UV–visible spectroscopy. UV– visible spectra of as-synthesised (in n-hexane) and phase transferred (in water) SNPs were recorded on Hitachi U-3900H double beam UV–visible spectrophotometer. Hydrodynamic size and size distribution of SNPs was obtained by dynamic light scattering. The measurements were carried out on Brookhaven 90Plus Particle Size Analyser at 25°C. Transmission electron microscopy (TEM) was performed on Philips CM200 TEM at an accelerating voltage of 200 kV. Sample for TEM was prepared by placing a drop of the colloidal dispersion of SNPs in n-hexane onto an amorphous carbon-coated copper grid. n-Hexane wasallowed to evaporate slowly at 25°C. The size-distribution histogram was prepared by measuring the diameter of 100 particles from TEM micrograph. To understand the surface functionalisation of antibiotics on SNPs, Fourier transform infrared (FTIR) spectroscopy was used. FTIR spectra of antibiotics andantibiotics adsorbed SNPs were recorded on Bruker Vertex 80 FTIR spectrophotometer in the mid infrared region (4000– 400 cm^{-1}) by using diamond attenuated total reflection (ATR) accessory. Concentration of silver in aqueous dispersion was measured by inductively

coupled plasma atomic emission spectroscopy (ICP-AES). The measurements were performed on Spectro's ARCOS ICP-AES.

ANTIBIOTIC CONTENT Antibiotic content and antibiotic loading of antibiotics in antibiotic adsorbed SNPs were determined by UV–visible spectroscopy. Optical density of antibiotics that remained unincorporated (supernal) with SNPs was measured at 276 nm for tetracycline and at 256 nm for kanamycin and its concentration was determined by Beer–Lambert law, $A = \varepsilon cl$; where A is the optical density at sample concentration c, l is the path length of sample cell (10 mm) and ε is the molar absorptivity (ε for tetracycline is $14.58 \times 10^6\ M^{-1}\ cm^{-1}$ and for kanamycin is $143.40\ M^{-1}\ cm^{-1}$) of the drug. Antibiotic content and antibiotic loading efficiency were determined by using the following expressions [29]

$$\text{Antibiotic content} = \frac{\text{Weight of antibiotic adsorbed on nanoparticles}}{\text{Total weight of nanoparticles}} \times 100$$

$$\text{Antibiotic loading efficiency} = [(W_1 - W_2)/W_1] \times 100$$

where W_1 is the total weight of antibiotic and W_2 is the weight of free antibiotic, which did not adsorb on nanoparticles.

ANTIBACTERIAL ACTIVITY OF SNPS

Antimicrobial activities of SNPs were evaluated in terms of MIC (minimum inhibitory concentration) and ZIH (zone of inhibition) measurements. MIC was measured by micro-dilution method, while ZIH was obtained from Kirby–Bauer (disk diffusion) assay. Both micro-dilution and disk diffusion tests were performed on clinically important pathogenic (*S. aureus*, *B. megaterium*,*P. vulgaris* and *S. sonnei*) and non-pathogenic (*B. subtilis* and*P. fluorescens*) strains.

In the micro-dilution test, six sets of 10 mL nutrient broth medium containing SNPs with effective silver concentration of 0–200 μg/mL were prepared. Each set was inoculated aseptically with 10^8 CFU/mL of the respective bacterial suspension. The inoculated sets were incubated at 37°C for 24 h. Each experiment was performed in triplicate. MIC was measured by visual inspection of growth or no growth of bacterial strain in the test tubes containing different
concentrations of SNPs. The lowest concentration of SNPs that inhibited bacterial growth was taken as the MIC for that particular bacterium. Control experiments were also run parallel to investigate the antibacterial activities of nutrient broth medium.

ZIH was measured for each bacterial strain by the Kirby–Bauer
method. ZIH is the area on the agar plate where the by antibacterial agen Equal volume of Mueller–Hinton agar medium was poured into a disposable petri dish. The medium was allowed to solidify. The bacterial strain was inoculated onto the entire surface of a Mueller–Hinton agar plate with the help of sterile cotton-tipped swab to form an even lawn. The sample disk containing 30 μg of antibacterial agent (SNPs/ tetracycline/kanamycin/tetracycline adsorbed SNPs/kanamycin adsorbed SNPs) was put on every plate. Each experiment was carried out in triplicate and results were statically averaged. Each set was incubated at 37°C for 24 h and ZIH was measured after the incubation period.

Results and discussion

Investigation of SNPs

UV–visible spectra of SNPs recorded before and after the phase transfer are shown in Fig. 1. A single plasmon band was observed both before and after the phase transfer. Observation of single SPR band in the UV–visible spectra of phase transferred SNPs indicates that the particle morphology is not affected by the phase transfer. The SPR band after the phase transfer shows a red shift. This might be due to the difference in surface adsorbed species on SNPs and medium of dispersion before and after the phase transfer [30].

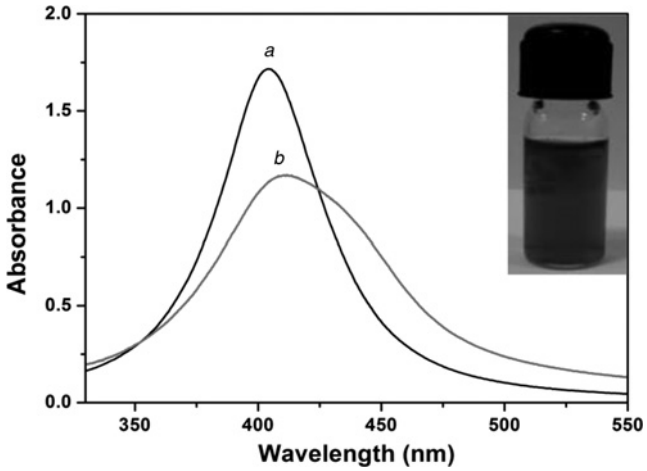

Fig. 2*a* shows the TEM micrograph of as-synthesised SNPs. Nanocrystals of silver self-assembled into the regular hexagonal closed pack lattice. Each particle has spherical morphology. No aggregation was observed. Size distribution histogram (Fig. 2*b*) was prepared by measuring the diameter of at least 100 particles. The histogram was fitted with lognormal particle size distribution function [31]. The average physical size and polydispersity index obtained from the fit are 8.07 ± 0.2 nm and 0.17 ± 0.03, respectively. Low value of polydispersity index confirms that the synthesised SNPs are monodisperse in size. Selected area electron diffraction pattern of SNPs is also shown as an inset in Fig. 2*b*. Four well resolved diffraction rings corresponding to (111), (200),(220) and (311) lattice planes of FCC crystal were observed.The hydrodynamic particle size distribution of SNPs recorded before and after the phase transfer is shown in Fig. 3. Each histogram was fitted with lognormal particle size distribution function [31]. The mean hydrodynamic size was 10.2 ± 0.2 nm (before the phase transfer) and 59 ± 0.14 nm (after the phase transfer), respectively. An increase in the hydrodynamic size of SNPs after their phase transfer is because of the difference in the hydrodynamic size of surface adsorbed species [32]. The mean hydrodynamic size (10.2 nm) of as-synthesised SNPs (in n-hexane) is greater than its physical size (8.07 nm) obtained

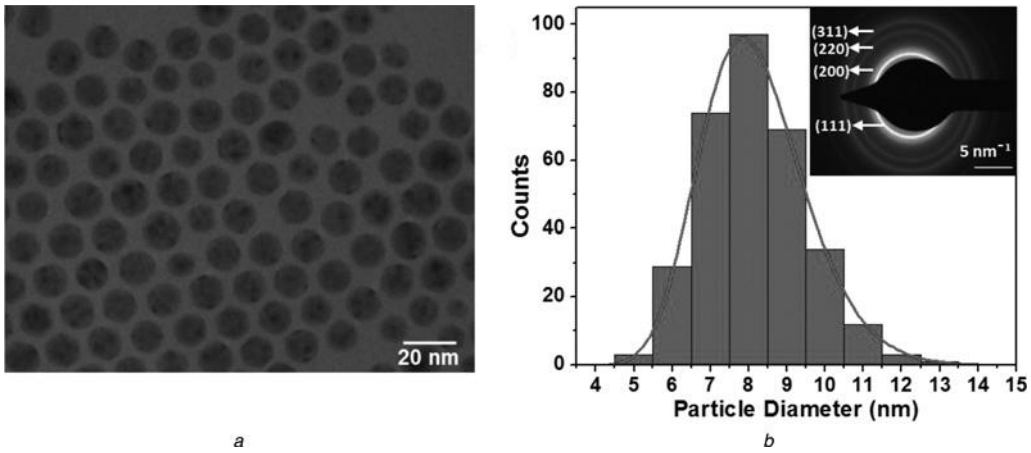

Fig. 2 *TEM of SNPs*

Fig. 3 Hydrodynamic size distribution histograms of SNPs (a) before and

(b .after stage move. Every histogram is fitted with lognormal molecule size circulation functionfrom transmission electron microscopy. This is clear as hydrodynamic size represents both the center and the covering. The chain length of a monomer of oleylamine is 1.9 nm, which represents the contrast between the actual size and hydrodynamic size of SNPs (before stage move) got from TEM and dynamic light dispersing, individually. To comprehend the impact of development media on the collection qualities of SNPs, their hydrodynamic size and polydispersity was estimated for 20 min. It has been discovered that the hydrodynamic size of SNPs in the development media increments significantly regarding their hydrodynamic size in water. The hydrodynamic size after 20 min increments to 91.5 nm (in development media) from 59 nm (in water) with expanded polydispersity from 0.13 of 0.34. These adjustments in the size a lot appropriation of SNPs are a direct result of the modification of the surface properties of SNPs in the development medium, which prompts their total. 2a shows the TEM micrograph of as-orchestrated SNPs. Nanocrystals of silver self-gathered into the ordinary hexagonal shut pack cross section. Every molecule has round morphology. No conglomeration was noticed. Size dissemination histogram (Fig. 2b) was set up by estimating the width of at any rate 100 particles. The histogram was fitted with lognormal molecule size appropriation work [31]. The normal actual size and polydispersity file acquired from the fit are 8.07 ± 0.2 nm and 0.17 ± 0.03, individually. Low estimation of polydispersity list confirms that the combined SNPs are monodisperse in size. Chosen region electron diffraction example of SNPs

is additionally appeared as an inset in Fig. 2b.

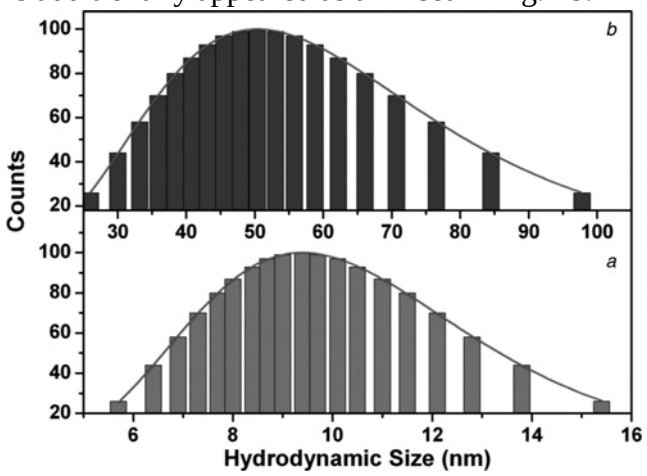

Fig. 3 *Hydrodynamic size distribution histograms of SNPs (a) before and*

(b) after phase transfer. Each histogram is fitted with lognormal particle size distribution function

Antibiotics adsorption on SNPs

Interaction of antibiotics with SNPs was studied by UV–visible and FTIR spectroscopy. UV-visible absorption spectra of tetracycline, tetracycline adsorbed SNPs and kanamycin, kanamycin adsorbed SNPs are shown in Fig. 4. Tetracycline has three characteristics absorption bands in its UV–visible spectrum at 250, 275 and357 nm. They correspond to $\pi \rightarrow \pi^*$ transitions of C=C. Kanamycin has no characteristic absorption band in the UV–visible region, but its complex with copper shows characteristics absorption at 256 nm. To monitor kanamycin, we have prepared solution of kanamycin in copper containing aqueous medium. UV–visible spectrum of this is shown in Fig. 4. In case of tetracycline adsorbed SNPs, multiplets of tetracycline are shifted to 252, 272 and 374 nm. The SPR due to SNPs has been red shifted from 428 to 435 nm. In case of kanamycin adsorbed SNPs, the characteristic absorption of kanamycin at 256 nm has been shifted to 252 nm while the SPR band of SNPs is shifted to 430 nm. Slight blue shifts in the spectral signatures of tetracycline, kanamycin and SNPs indicate the physisorption of antibiotics on SNPs.Physisorption of antibiotics on SNPs is further confirmed by FTIR spectroscopy. It is a powerful technique used to understand surface functionalisation of nanoparticles. In Fig. 5, FTIR spectra of tetracycline, tetracycline adsorbed SNPs, kanamycin and kanamycin adsorbed SNPs are shown. No major peak shift in the fingerprint region of the FTIR spectra of tetracycline or kanamycin has been observed when they adsorbed on the surface of SNPs,which further strengthen our claim that the antibiotics are physisorbed on nanoparticles' surface.

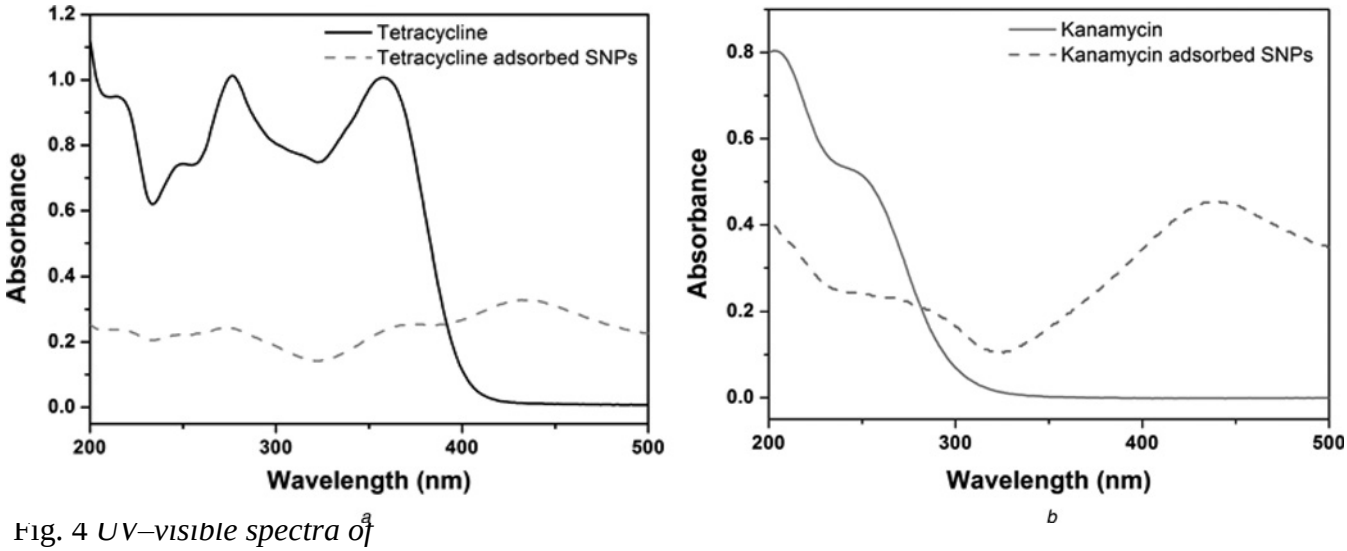

Fig. 4 *UV–visible spectra of*

a Tetracycline (line) and tetracycline adsorbed SNPs (small dashed line);

b Kanamycin (line) and kanamycin adsorbed SNPs (small dashed line).

Slight blue shift in the characteristics absorption peaks of tetracycline adsorbed SNPs and kanamycin adsorbed SNPs shows that antibiotics are physisorbed on the surface of SNPs

Antibiotic content and antibacterial activity

Antibiotic content and antibiotic loading were determined from UV– visible spectroscopy. The loading efficiency of tetracycline was 15.3% and drug content was 40.56%. For kanamycin, the loading efficiency was 6.44% and the drug content was 90.40%. Antibacterial activity of SNPs was evaluated against four pathogenic (*S. aureus*, *B. megaterium*, *P. vulgaris* and *S. sonnei*) and two non-pathogenic (*B. subtilis* and *P. fluorescens*) strains by micro-dilution and Kirby–Bauer tests. From micro-dilution method, the MIC values of pluronic F-127 stabilised SNPs were determined. To further understand the effectiveness of antibacterial agents on pathogenic microorganisms, the ZIH was measured by Kirby–Bauer test. The MIC values of SNPs for the bacterial strains under investigation are reported in Table 1. The MIC value of SNPs is 75 µg/mL for *B. megaterium* followed by 100 µg/mL for *P. vulgaris* and *S. sonnei* and 150 µg/mL for *S. aureus*. Fornon-pathogenic strains, these MIC values are 25 µg/mL each for*B. subtilis* and *P. fluorescens*.

Results of antimicrobial tests of SNPs by Kirby–Bauer method are shown in Fig. 6 and summarised in Table 1. To understand the synergistic effect of SNPs on antibacterial activities of commercial antibiotics, the Kirby–Bauer test was also performed on tetracycline adsorbed SNPs and kanamycin adsorbed SNPs. An increase in the inhibition zone was found to be in the range of 0– 346% for microorganisms under investigation when tetracycline was adsorbed on SNPs. The ZIH increases by 110–289% when kanamycin adsorbed on SNPs. The % increase in ZIH values was determined by applying the correction for effective antibiotic content (15.3% for tetracycline and 6.44% for kanamycin) in antibiotic adsorbed SNPs. The synergistic effect of SNPs is clearly evidenced by the percentage increase in ZIH for antibioticadsorbed SNPs with respect to the inhibition zone found for antibiotic.Results of micro-dilution and Kirby–Bauer tests show strong biocidal activities of SNPs and antibiotic adsorbed SNPs. The exact mechanism responsible for this bactericidal action of SNPs and its synergistic effect on commercial antibiotics is not well understood. Various possible modes of

biocidal action of metal nanoparticles were proposed in the literature [33–38]. Poisoning of bacterial cell by antibiotic adsorbed SNPs is a multi-step process. In the first step, antibacterial agent internalises into the bacterial cell. Nanoparticles diffuse into the bacterial cell by ion-transport proteins [34]. Some nanoparticles also enter into the bacterial cell by endocytosis [35]. The bacterial cell wall is composed of thick peptidoglycan layer linked to teichoic acid that gives negative charge to the cell wall. The negative charge facilitates the interaction between the cell wall and positively charged metal. Interaction between metal ion and bacterial cell wall causes the loss of membrane integrity. The damaged membrane allows the entry of substances from the environment (traditional antibiotics in our case), which causes osmotic imbalance. The damaged cellmembrane also allows the leakage of minerals and genetic materials. The leakage of cytoplasmic content and consequent rupture of the cell leads to its death.

In the second step, internalised nanoparticles and antibiotics induce toxicity by reactive oxygen species (ROS) mediated cellular damage or because of the metal catalysed oxidation reaction that could underline specific proteins, membrane or DNA damage. Increasing ROS level in the cellular environment leads to the rapid degradation of cellular contents that eventually leads to the cell death [35]. Another possibility is the formation of protein disulphides and depletion of antioxidant reserves [36]. This is because of the formation of covalent bonds between metal ions and S. This depletion in antioxidant reserves can leave protein targets vulnerable to attack by metal ions or ROS. It also prevents repair of oxidised protein and thus enhances the possibility of oxidative stress induced cellular damaged in bacteria [36]. Metal nanoparticles can induce toxicity to bacterial cells by protein dysfunction. Amino acid residue in proteins is susceptible to metal-catalysed oxidation [37]. Oxidation of amino acid side chains in proteins can cause loss of catalytic activity and triggerprotein degradation [37]. This degradation might also be responsible for the nanoparticle toxicity.

The observed toxicity is also linked to starvation-induced growth arrest. SNPs inhibit the uptake of sulphate and deplete intracellular S metabolite pool [38]. Due to supplementation with sulphate and other S sources mitigates toxicity in a concentration dependent manner, it has been suggested that SNPs starve cells of S by interfering with its sulphate uptake and thus induce cell apoptosis. The presence of metal nanoparticles and conventional antibiotics in bacterial medium execute these modes simultaneously. The growth inhibition and cellular death of bacterial cells are due to combination of these mechanisms.

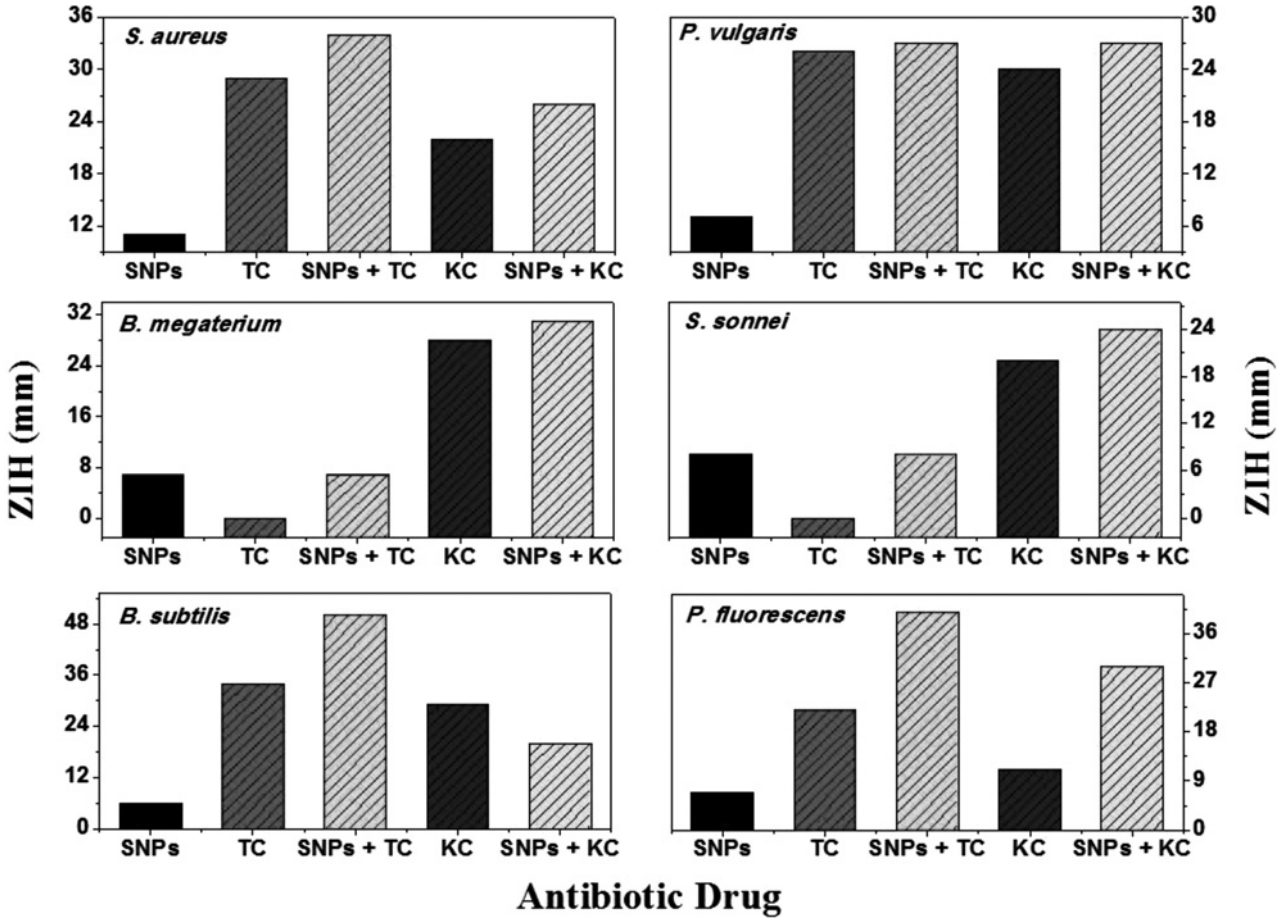

Conclusion

Antibiotic adsorption on SNPs enhances the biocidal activities of conventional antibiotics. The antimicrobial efficiency of tetracycline increases by 0–346% when adsorbed on SNPs, while for kanamycin; the increase is in the range of 110–289%. Theobserved synergies between conventional antibiotics and SNPs in their biocidal activities against pathogenic and non-pathogenic microorganisms are because of execution of various modes of biocidal action of metal nanoparticles and conventional antibiotics, simultaneously.

REFERENCE

1 Reese, R.E., Betts, R.F., Gumustop, B.: 'Handbook of antibiotics' (The Lippincott Williams & Wilkins Handbook Series, 1993, 3rd edn.)

2 Moran, L.F., Aronsson, B., Manz, C., et al.: 'Critical shortage of new antibiotics in development against multidrug-resistant bacteria-Time to react is now', Drug Resist. Updat., 2011, 14, pp. 118–124

3 Batabyal, P., Mookerjee, S., Sur, D., et al.: 'Diarrheogenic Escherechia coli in potable water sources of West Bengal, India', Acta Trop., 2013, 127, pp. 153–157

4 Hui, C., Lin, M.C., Jao, M.S., et al.: 'Previous antibiotic exposure and evolution of antibiotic resistance in mechanically ventilated patients with nosocomial infections', J. Crit. Care, 2013, 28, pp. 728–734

5 Granowitz, E.V., Brown, R.B.: 'Antibiotic adverse reactions and drug interactions', Crit. Care Clin., 2008, 24, pp. 421–442

6 Tan, H., Ma, C., Song, Y., et al.: 'Determination of tetracycline in milk by using

nucleotide/lanthanide coordination polymer-based ternary complex', Biosens. Bioelectron., 2013, 50, pp. 447–452
7 Grill, M.F., Maganti, R.K.: 'Neurotoxic effects associated with antibiotic use: management considerations', Br. J. Clin. Pharmacol., 2011, 72, pp. 381–393
8 Varkey, A.J.: 'Antibacterial properties of some metals and alloys in combating coliforms in contaminated water', Sci. Res. Essays, 2010, 5, pp. 3834–3839
9 Rizzo, L., Sannino, D., Vaiano, V., et al.: 'Effect of solar simulated N-doped TiO_2 photocatalysis on the inactivation and antibiotic resistance of an E. coli strain in biologically treated urban waste water', Appl. Catal. B, Environ., 2014, 144, pp. 369–378
10 Yasuyuki, M., Kunihiro, K., Kurissery, S., et al.: 'Antibacterial properties of nine pure metals: a laboratory study using Staphylococcus aureus and Escherichia coli, ' Biofouling, 2010, 26, pp. 851–858
11 Loomba, L., Scarabelli, T.: 'Metallic nanoparticles and their medicinal potential. Part II: aluminosilicates, nanobiomagnets, quantum dots and cochleates', Ther. Deliv., 2013, 4, pp. 1179–1196
12 Shanmugasundaram, T., Radhakrishnan, M., Gopikrishnan, V., et al.: 'A study of the bactericidal, anti-biofouling, cytotoxic and antioxidant properties of